journal of the mechanical behavior of biomedical materials 157 (2024) 106642

Contents lists available at ScienceDirect

Journal of the Mechanical Behavior of Biomedical Materials

journal homepage: www.elsevier.com/locate/jmbbm

Mechanical and biological behavior of double network hydrogels reinforced with alginate versus gellan gum

Alaa Ajam [a], Yuwan Huang [a], Md Shariful Islam [b], Kristopher A. Kilian [b,c], Jamie J. Kruzic [a,*]

[a] School of Mechanical and Manufacturing Engineering, University of New South Wales (UNSW Sydney), Sydney, NSW, 2052, Australia
[b] School of Materials Science and Engineering, University of New South Wales (UNSW Sydney), Sydney, NSW, 2052, Australia
[c] School of Chemistry, Australian Centre for NanoMedicine, University of New South Wales (UNSW Sydney), Sydney, NSW, 2052, Australia

ARTICLE INFO

Keywords:
Double network hydrogels
Alginate
Gellan gum
Polyethylene glycol
Mechanical properties
Adipose derived stromal cells

ABSTRACT

Alginate and gellan gum have both been used by researchers as reinforcing networks to create tough and biocompatible polyethylene glycol (PEG) based double network (DN) hydrogels; however, the relative advantages and disadvantages of each approach are not understood. This study directly compares the mechanical and biological properties of polyethylene glycol di-methacrylate (PEGDMA) hybrid DN hydrogels reinforced with either gellan gum or sodium alginate using PEGDMA concentrations from 10 to 20 wt% and reinforcing network concentrations of 1 and 2 wt%. The findings demonstrate that gellan gum reinforcement is more effective at increasing the strength, stiffness, and toughness of PEGDMA DN hydrogels. In contrast, alginate reinforcement yields DN hydrogels with greater stretchability compared to gellan gum reinforced PEGDMA. Furthermore, separate measurements of toughness via unnotched work of rupture testing and notched fracture toughness testing showed a strong correlation of these two properties for a single reinforcing network type, but not across the two types of reinforcing networks. This suggests that additional notched fracture toughness experiments are important for understanding the full mechanical response when comparing different tough DN hydrogel systems. Regarding the biological response, after conjugation of matrix protein to the surface of both materials robust cell attachment and spreading was supported with higher yes associated protein (YAP) nuclear expression observed in populations adhering to the stiffer gellan gum-PEGDMA material. This study provides valuable insights regarding how to design double network hydrogels for specific property requirements, e.g., for use in biomedical devices, as scaffolding for tissue engineering, or in soft robotic applications.

1. Introduction

Hydrogels have received strong interest in the field of biomedical materials due to their 3D hydrophilic structure that has the capacity to absorb large amounts of water or biological fluids. Prominent among these applications are contact lenses, wound dressing, drug delivery devices, tissue engineering scaffolds, and hygiene products (Caló and Khutoryanskiy, 2015; Lin and Metters, 2006; Lin and Anseth, 2009; Peppas et al., 2000). In this context, polyethylene glycol (PEG) based hydrogels have excellent characteristics for biomedical applications such as high hydrophilicity coupled with high biocompatibility for cells and biomolecules (Lin and Anseth, 2009). Furthermore, the mechanical characteristics of PEG based hydrogels can be tailored for specific applications by controlling the molecular weight and concentration of the monomers utilized in their formulation (Huang et al., 2022; Lee et al., 2014; Nguyen et al., 2012). However, long-standing shortcomings of PEG based hydrogels have been their low strength and toughness.

For the field of hydrogel materials to expand to encompass load-bearing biomedical applications and soft robotics, including artificial muscles, nerves, and cartilage (Huey et al., 2012; Matsuda et al., 2019), hydrogel materials with high strength and toughness are required. To fill this need, various types of double network (DN) hydrogels have been developed with exceptional strength, stretchability, and toughness (Pacelli et al., 2014; Trucco et al., 2021; Zhou et al., 2019, 2020). This approach has been applied extensively to biocompatible PEG-based hydrogels and sodium alginate (Al) and gellan gum (GG) serve as notable examples of reinforcing networks used to strengthen, stiffen, and toughen DN PEG-based hydrogels (Hong et al., 2015; Huang et al., 2022; Li et al., 2020; Pacelli et al., 2014; Trucco et al., 2021; Zhou et al., 2019, 2020). Alginate and gellan gum single network hydrogels both

* Corresponding author.
E-mail address: j.kruzic@unsw.edu.au (J.J. Kruzic).

https://doi.org/10.1016/j.jmbbm.2024.106642
Received 2 April 2024; Received in revised form 6 June 2024; Accepted 22 June 2024
Available online 25 June 2024

utilize ionic interactions in the presence of multivalent ions, and they possess attractive properties such as ductility, self-healing, and biocompatibility (Lee and Mooney, 2012; Zia et al., 2018). Due to those attractive properties, both have garnered significant attention as reinforcing networks for creating tough, stretchable, and biocompatible DN PEG-based hydrogels.

While both alginate and gellan gum have been used successfully as reinforcing networks in the preparation of double network PEG-based hydrogels, to date little is known about the comparative advantages and disadvantages in choosing one relative the other. Thus, it remains unclear what unique characteristics each provides the DN hydrogels in terms of their mechanical properties, as well as the appropriate choice of reinforcing network for specific target applications. To address this issue, the present study compares the mechanical properties of alginate and gellan gum reinforced double network PEG-based hydrogels over a range of polymer network concentrations. Adipose derived stromal cells (ADSCs) are then cultured on selected DN hydrogels to demonstrate cytocompatibility and compare the cell responses to each reinforcing network type. The results of this work provide some key design principles for developing strong and tough hybrid DN hydrogels suitable for various applications.

2. Materials and methods

2.1. Materials

To create the covalently bonded networks, linear 10 kDa PEGDMA was synthesized using a process described previously (Huang et al., 2022; Islam et al., 2021). In brief, a solution of 10 kDa polyethylene glycol (PEG) purchased from Sigma-Aldrich was dissolved in toluene and dehydrated twice using an evaporator. The dehydrated PEG was then dissolved in toluene, dichloromethane, and triethylamine to react with 2.2 equivalents of methacrylic anhydride. The reaction mixture was allowed to stir for 48 h at room temperature. Then, the reaction was quenched with sodium bicarbonate. Diethyl ether was added to filter and precipitate the PEGDMA, followed by vacuum filtration. The obtained PEGDMA was stored at −20 °C for further use. 2-hydroxy-4′-(2-hydroxyethoxy)-2-methylpropiophenone (Irgacure 2959) was used as the photoinitiator and was purchased from Sigma-Aldrich Australia. To create the ionically bonded reinforcing networks, sodium alginate (Al) and gellan gum (GG) were purchased from ChemSupply Australia. Additionally, calcium chloride obtained from ChemSupply Australia was used for the ionic crosslinking of the hydrogels.

2.2. Preparation of alginate reinforced PEGDMA double network hydrogels

Alginate (Al) solutions and PEGDMA solutions were prepared by dissolving Al and PEGDMA, respectively, in deionized water by magnetic stirring for 15 min. Following this, the alginate and PEGDMA solutions were combined to give the final concentrations shown in Table 1 and stirred for an additional 15 min.

The photoinitiator, Irgacure 2959, was dissolved in 100 % (v/v) ethanol to create a 1 M solution. This solution was then added to the previous mixture at a concentration of 50 μl for every 0.01 mmol of PEGDMA. The resulting solution was poured into an open mold composed of either a dog-bone shaped or rectangular shaped silicon sheet with a thickness of 1 mm placed on top of a glass sheet. The mold was closed using another glass sheet and the assembly was held together with clips.

Lastly, the samples were subjected to irradiation using a Spectrolinker XL-1000 UV crosslinker for 1 h to form gel sheets. The gel sheets were subsequently soaked in a 0.1 M $CaCl_2$ solution for 1 h to accomplish the ionic crosslinking of the alginate, thus forming the second network.

2.3. Preparation of gellan gum reinforced PEGDMA double network hydrogels

Gellan gum (GG) solutions and PEGDMA solutions were prepared by dissolving GG and PEGDMA, respectively, in deionized water by magnetic stirring at 60 °C for 30 min. Subsequently, the solutions were mixed to give the final concetrations shown in Table 1 by magnetic stirring for an additional 30 min while maintaining 60 °C temperature control.

The 1M photoinitiator solution was prepared following the previously described method and added to the mixed solutions at a concentration of 50 μl for every 0.01 mmol of PEGDMA while maintaining stirring at 60 °C for an additional 15 min.

The gel formation process proceeded in the same manner as described for the preparation of alginate reinforced PEGDMA hydrogels, where the PEGDMA network was first formed by applying irradiation and soaking in the $CaCl_2$ solution was used to form the second network. Table 1 gives a summary of all the prepared double network hydrogels.

2.4. Gel swelling

After removing the hydrogel samples from the $CaCl_2$ solution, any excess liquid was carefully dried using tissue paper and the mass was measured (m_i). Then, the samples were immersed in 10 ml of 0.1 M $CaCl_2$ solution overnight to allow for swelling and the mass (m_s) of each swollen gel sample was measured again before mechanical testing. The weight difference method was employed to calculate the swelling ratio, S, for each sample as follows (Pal et al., 2009):

$$S(\%) = \frac{m_s - m_i}{m_i} \times 100, \quad (1)$$

where m_s is the mass of hydrogel in the swollen state and m_i is the mass of hydrogel in the initial as-prepared state. To model the mechanical properties, the swelling stretch of the hydrogels was calculated as the change in gauge width of the dog-bone shaped samples, $\frac{W_s}{W_i}$, where W_s is the gauge width in swollen state and W_i is the gauge width in initial as-prepared state (Uchida et al., 2019).

2.5. Tensile testing

Uniaxial tensile tests were conducted using a Mark-10 ESM 303 testing machine equipped with a calibrated 100 N load cell to evaluate the mechanical properties of dog-bone shaped samples for all DN hydrogels listed in Table 1. For each group, four dog-bone shaped samples were subjected to stretching until failure, using a stretching rate of 0.5 mm/min. To enable gripping in the tester, the 1 mm thick hydrogel samples were affixed between two polypropylene sheets along with a silicon spacer. The spacer was positioned approximately 2–3 mm from the end of the hydrogel samples, as shown in Fig. 1a. Cyanoacrylate adhesive was used to securely attach the samples to the sheets. Then, the samples were clamped at the spacer area to avoid damaging the hydrogel samples. Additionally, to understand the relative strain rate sensitivity of Al and GG reinforced hydrogels, the 10 wt% PEGDMA + 1 wt.% Al and 10 wt% PEGDMA + 1 wt.% GG DN hydrogel groups were also tested at a higher strain rate of 5 mm/min for comparison. A load-displacement curve was obtained for each tested sample.

The axial strain could not be calculated directly from the displace-

Table 1
Compositions of the various double network hydrogels.

10 kDa PEGDMA	Reinforcing Networks: Alginate (Al) or Gellan Gum (GG)			
10 wt%	+1 wt% Al	+2 wt% Al	+1 wt% GG	+2 wt% GG
15 wt%	+1 wt% Al	+2 wt% Al	+1 wt% GG	+2 wt% GG
20 wt%	+1 wt% Al	+2 wt% Al	+1 wt% GG	+2 wt% GG

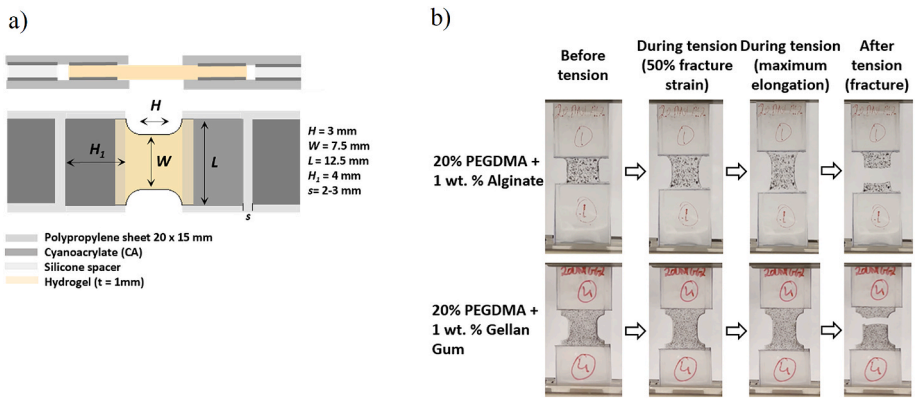

Fig. 1. a) The dog-bone sample design used for tensile testing. b) Photos taken during tensile testing showing the stretching of 20 wt% PEGDMA + 1 wt.% Al and 20 wt% PEGDMA + 1 wt.% GG DN hydrogel samples.

ment data since it is related to the displacement of the whole sample rather than the gauge length. To accurately calculate the axial strain within the gauge length, 2D digital image correlation (DIC) was employed. A black speckle pattern was spray painted onto the surface of each sample to enable tracking of displacement points within the gauge length (Fig. 1b). Videos of the tension tests were recorded to track the speckles until sample failure and a custum MATLAB code was used to extract two images per second from the videos. Image data were then imported into GOM software to track the displacement of two points within the gauge length to create a virtual extensometer and obtain the axial displacement data. A correlation between the axial displacement data and the load vs. time record was made for each sample to generate a stress-strain curve for the determination of the elastic modulus, failure stress, failure strain, and work of rupture. The engineering strain and stress were calculated as $\varepsilon_e = \frac{\Delta l}{l_0}$ and $\sigma_e = \frac{F}{A_0}$, respectively where ε_e is the engineering strain, Δl is the displacement, l_0 is the initial gauge length, σ_e is the engineering stress, F is the load, and A_0 is the initial area of the cross section. True stress and strain were calculated as $\varepsilon_t = \ln(1+\varepsilon_e)$ and $\sigma_t = \sigma_e(1+\varepsilon_e)$. The elastic modulus E was calculated by linear fitting the true stress-strain data over the region of 5–10 % strain for each stress-strain curve. The work of rupture was calculated as the area under the true stress-strain curve up to the failure point.

2.6. Mechanical modelling

The Arruda and Boyce (1993) model was fit to the experimental stress-stretch data to aid in interpreting how the PEGDMA and reinforcing network concentrations affect the various mechanical properties by affecting the network structure. The mechanical model is derived based on material constants "n" and "N," which represent the effective network crosslink density and the effective number of Kuhn segments between crosslinks, respectively.

The stress-stretch relation is expressed as:

$$\sigma_t = \frac{nkT}{3}\frac{N}{\lambda_{ch}}\mathscr{L}^{-1}\left[\frac{\lambda_{ch}}{\sqrt{N}}\right]\left(\lambda^2 - \frac{1}{\lambda}\right), \tag{2}$$

where k is Boltzmann's constant, T is the temperature, $\mathscr{L}^{-1}$ is the inverse Langevin function, $\lambda = 1 + \varepsilon_e$ is the stretch, and λ_{ch} is the chain stretch which is expressed as:

$$\lambda_{ch} = \frac{1}{\sqrt{3}}\sqrt{\lambda^2 + \frac{2}{\lambda}}. \tag{3}$$

The stress-stretch data obtained for the samples were analyzed by fitting them to the Arruda-Boyce model (Eq. (2)) using the least-squares method in MATLAB code. The model parameters for all of the swollen double network hydrogels were calculated. Subsequently, the material constants of the as-prepared hydrogels were calculated by adjusting the swollen parameters using the swelling stretch, λ_s, according to the following equations (Uchida et al., 2019):

$$n_{as-prepared} = n_{swollen}(\lambda_s)^3, \tag{4}$$

$$N_{as-prepared} = N_{swollen}(\lambda_s)^2. \tag{5}$$

2.7. Fracture toughness testing

The critical energy release rate (Γ) was utilized to determine the fracture toughness of the hydrogels using the "pure shear" test method developed by Rivlin and Thomas (1953). This method requires testing both notched and unnotched rectangular samples under tension loading to failure. The critical energy release rate can be calculated as:

$$\Gamma = H\,W(\lambda_c), \tag{6}$$

where H is the distance between the two grippers, $W(\lambda_c)$ is the energy density calculated as the area under the stress-stretch curve of an unnotched sample from $\lambda = 1$ to λ_c, and λ_c is the critical stretch that is obtained when the crack starts to grow in the notched samples.

Both notched and unnotched "pure shear" tensile tests were conducted using a Mark-10 ESM 303 test machine equipped with a calibrated 100 N load cell. The tests were performed using a stretching rate of 0.5 mm/min. The unnotched hydrogel samples had dimensions of 20 mm in length, 18 mm in width, and 1 mm in thickness. Notched samples were prepared by creating a single 9 mm notch in the width direction at

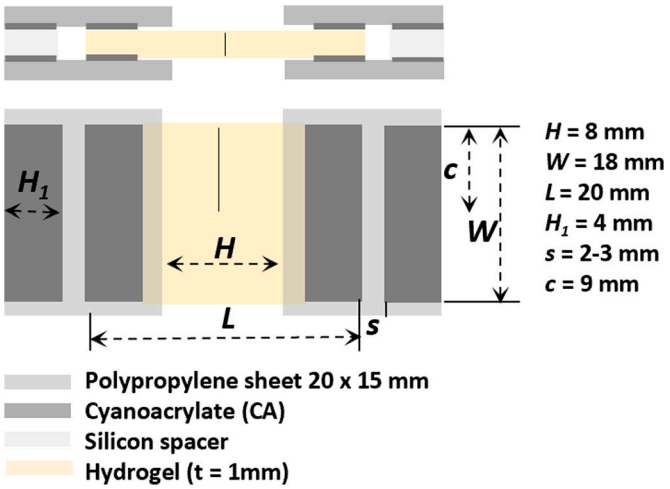

Fig. 2. The notched sample design used for fracture toughness testing.

the center of the sample using a razor blade as shown in Fig. 2.

Both unnotched and notched samples were glued together with a silicon spacer between two polypropylene sheets using cyanoacrylate adhesive while ensuring a gap distance of approximately 2–3 mm from the end of the hydrogel samples to the spacer as shown in Fig. 2. During testing, the samples were gripped at the spacer area. One unnotched and four notched samples were tested from each group.

2.8. Cell culture experiments

To assess the relative biocompatibility of representative DN hydrogel groups reinforced with alginate or gellan gum, samples were prepared with an approximate thickness of 1 mm following the previous protocol for the compositions 10 wt% PEGDMA + 1 wt.% Al and 10 wt% PEGDMA + 1 wt.% GG. Fibronectin was chemically conjugated into the alginate and gellan gum networks to enhance cell adhesion, employing carbodiimide chemistry following a protocol from the literature (Ferris et al., 2015; Rowley et al., 1999). First, the hydrogel sheets were sectioned into rectangular samples measuring approximately 10 mm × 10 mm × 1 mm, subsequently placed into glass vials, and subjected to two rinses with 2-(N-morpholino)-ethanesulfonic acid (MES) buffer (pH = 5.5). Following this, the carboxylic acid groups of the alginate/gellan gum component were activated through the addition of water-soluble carbodiimide 1-ethyl-(dimethylaminopropyl) carbodiimide (EDC) (0.1 M), succeeded by N-hydroxysulfosuccinimide sodium salt (sulfo-NHS; 0.1 M), and then agitated for 20 min. Subsequently, fibronectin (50 mg/ml) was introduced into the glass vial with gentle agitation for 1 h. The resultant hydrogels underwent two washes with phosphate-buffered saline (PBS) before being transferred into a 12-well plate for cell seeding. Finally, the samples were rinsed again with sterile PBS and subjected to sterilization via UV exposure for 30 min.

Adipose-derived mesenchymal stem cells (ADSCs, ATCC PCS-500-011) were cultured in low-glucose Dulbecco's modified Eagle's medium (Thermo Fisher Scientific, Cat. No. 11885084), supplemented with 1 % (v/v) penicillin and streptomycin (Sigma Aldrich, Cat. No. P4333), and 10 % (v/v) fetal bovine serum (BOVO- GEN, Australia, Cat. No. SFBS-AU) under standard cell culture conditions (37 °C, 5 % CO_2, humidified incubator). The culture medium was refreshed every 48 h, and cells were passaged when reaching 80–85 % confluency. All ADSCs utilized in the experiments were at passage number 5.

To prepare the cells for analysis, ADSCs cultured on the DN hydrogel samples for 7 days were fixed with 4 % paraformaldehyde (Sigma-Aldrich Pty Ltd.) for 30 min, followed by permeabilization in 0.1 % Triton X-100 (Sigma-Aldrich Pty Ltd.) in PBS for 1 h. Blocking of the cells was achieved with 1 % bovine serum albumin (BSA) for 1 h. Immunolabeling of Yes-associated protein (YAP, 1:200) was conducted in 1 % BSA (w/v) in PBS for 24 h at room temperature, followed by two PBS rinses. Subsequently, secondary antibody labeling was carried out at a 1:500 dilution in 1 % BSA in PBS for 2 h at room temperature in the absence of light. Actin and nuclei were stained using 488-phalloidin (1:200) and Hoechst 33342 (1:1000), respectively. Immunofluorescence microscopy was performed using a Zeiss LSM 800 confocal microscope. Cell area analysis was accomplished by measuring the average cell area of 50 cells from three samples based on phalloidin staining of the actin cytoskeleton, utilizing ImageJ software. The determination of cell nuclear YAP localization percentages involved manual counting of cells exhibiting nuclear co-localized YAP, subsequently dividing by the total cell count, and multiplying by 100.

2.9. Statistical analyses

At least three replicates from each experimental group were utilized to calculate the swelling and mechanical properties of hydrogels. The data are presented as mean ± standard deviation. For statistical analysis comparing the alginate and gellan gum groups and assessing the impact of a higher concentration of reinforcing network on swelling ratio and mechanical properties, Levene's test revealed non-equal variances among many groups, thus, we conducted a Kruskal-Wallis test followed by Dunn's post-hoc analysis using SPSS software. Furthermore, to analyze the effect of the concentration of PEGDMA on the swelling ratio and mechanical properties, a linear regression was performed for each of the four groups (1 wt% Al, 2 wt% Al, 1 wt% GG, 2 wt% GG). For the regression analyses, the concentration of PEGDMA was utilized as the independent variable, while the type of the reinforcing network and its percentage were held constant. Finally, for the statistical analysis of the cell culture experiments a one-way analysis of variance (ANOVA) was performed. A p-value less than 0.05 was considered statistically significant for all statistical tests.

3. Results

3.1. Swelling properties

The swelling ratio results are presented in Fig. 3a with the numerical values summarized in Table S1 and the statistical test results summarized in Table S2−S4 of the supplementary data (Appendix A). It is evident that alginate double network (DN) hydrogels exhibit higher water absorption compared to gellan gum DN hydrogels ($p < 0.05$). The swelling ratios ranged from 5–30 % for alginate DN hydrogels and 1–10 % for gellan gum DN hydrogels. Increasing the concentration of the alginate reinforcing network leads to a significant reduction in the swelling ratio ($p < 0.05$), with no significant effect of gellan gum concentration ($p > 0.05$). The linear regression analyses revealed statistically significant linear relationships ($p < 0.05$) whereby increasing the concentration of PEGDMA increases the swelling ratio for all groups when holding the concentration and the type of the reinforcing network constant. Finally, the swelling stretch was consistently small (near 1.0) for all groups and there was no significant effect ($p > 0.05$) of any of the network variables (Fig. 3b).

3.2. Tensile testing

Representative tensile true stress-strain curves, which closely represent the average behavior of the alginate-PEGDMA and gellan gum-PEGDMA hybrid double network (DN) hydrogel groups, are presented in Fig. 4a and b, respectively. The average mechanical properties of all tested samples are presented in Fig. 5 with the numerical values summarized in Table S1 and the statistical test results summarized in Table S2−S4 of the supplementary data (Appendix A).

3.2.1. Comparisons for 1 wt% reinforcing network

As is seen in Fig. 5, the differences between using 1 wt% gellan gum versus alginate were somewhat less prominent than when using 2 wt%. Replacing 1 wt% of alginate with gellan gum gave significantly higher ($p < 0.05$) tensile strength, modulus, and fracture toughness, while the strain to failure was significantly lower. However, differences in the work of rupture were not statistically significant ($p > 0.05$) for the two reinforcing networks. Also, for the 1 wt% gellan gum samples increasing the PEGDMA content significantly increased most mechanical properties as revealed by statically significant ($p < 0.05$), positive linear correlations for most mechanical properties except for the strain to failure ($p > 0.05$). Finally, for the 1 wt% alginate samples only the modulus (increase) and strain to failure (decrease) were significantly ($p < 0.05$) affected when increasing PEGDMA content.

3.2.2. Comparisons for 2 wt% reinforcing network

As is seen in Fig. 5, increasing the concentration of alginate from 1 wt % to 2 wt% had a relatively small effect on the mechanical properties. However, an increase in the concentration of gellan gum from 1 wt% to 2 wt% significantly improved the tensile strength, modulus, strain, work of rupture, and fracture toughness. For the samples with 2 wt% of the reinforcing network, the differences between gellan gum and alginate

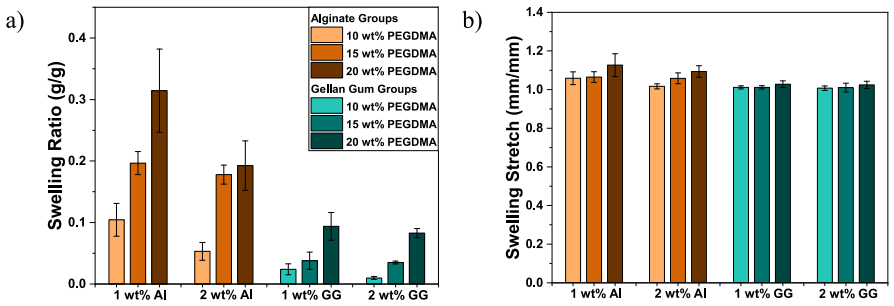

Fig. 3. a) Swelling ratios and b) swelling stretch for the different double network hydrogel groups.

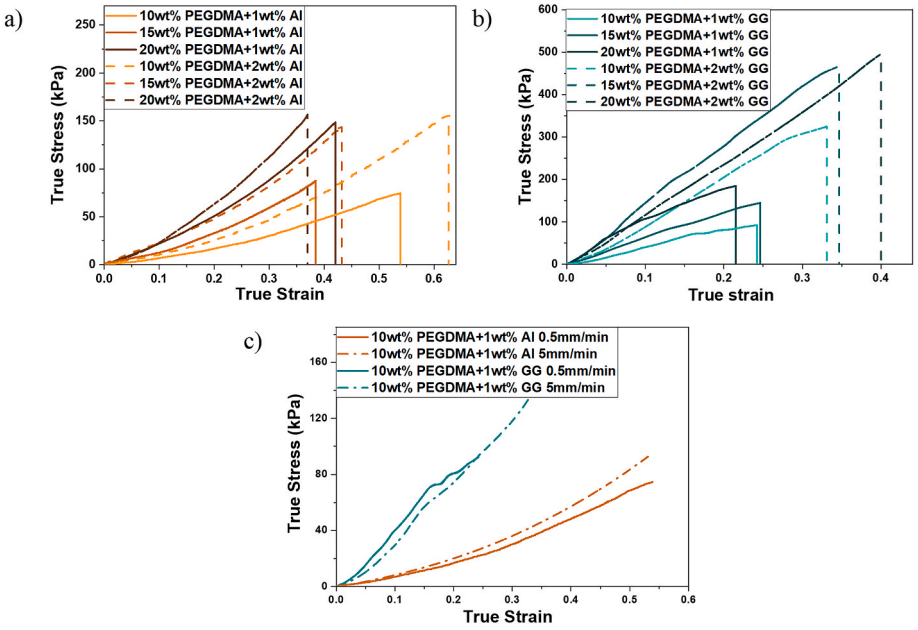

Fig. 4. True stress-strain curves of PEGDMA DN hydrogels reinforced with either a) alginate (Al) or b) gellan gum (GG) using a 0.5 mm/min displacement rate. c) Comparison of 10 wt% PEGDMA + 1 wt% Al and 10 wt% PEGDMA + 1 wt% GG DN hydrogels tested using 0.5 mm/min and 5 mm/min displacement rates.

were strong. Replacing 2 wt% of alginate with gellan gum gave significantly higher ($p < 0.05$) tensile strength, modulus, work of rupture, and fracture toughness, while the strain to failure was significantly lower. Also, for the 2 wt% gellan gum samples, increasing the PEGDMA content had the relatively strong effect of increasing all mechanical properties as revealed by statically significant ($p < 0.05$), positive linear correlations. In comparison, the effect of increasing PEGDMA content was less prominent for the 2 wt% alginate samples where the tensile strength and work of rupture were not significantly affected ($p > 0.05$). While the modulus significantly increased ($p < 0.05$) with increasing PEGDMA content, this had the trade-off of significantly lower ($p < 0.05$) fracture toughness and strain to failure.

3.2.3. *Effect of strain rate*

To investigate how strain rate influences the behavior of alginate and gellan gum hydrogels, two groups with 10 wt% PEDMA and 1 wt% reinforcing network were also tested at a stretching rate of 5 mm/min with the results for both stretching rates shown in Fig. 4c. The alginate group exhibited comparable responses under both stretching rates, whereas the gellan gum group displayed initially similar behavior but earlier failure under the higher strain rate (Fig. 4c). The mechanical properties for the alginate group remained almost identical under both strain rates (Table 2), as indicated by $p > 0.05$ results from the Kruskal-Wallis test. However, in the case of gellan gum, the failure stress, failure strain, and work of rupture (Table 2) were significantly higher at the higher strain rate ($p < 0.05$), with a slight decrease in the modulus ($p < 0.05$).

3.2.4. *Arruda-Boyce model fitting results*

Upon a visual comparison of the true stress-strain profiles for both the alginate (Fig. 4a) and gellan gum (Fig. 4b) groups with the Arruda-Boyce model, a distinct difference can be observed. The strain stiffening response up to the failure point of the alginate groups aligns well with the Arruda-Boyce model. Conversely, the gellan gum groups only exhibit strain stiffening up to a point, after which damage likely begins to initiate. To fit the behavior of the gellan gum hydrogels to the Arruda-Boyce model, a distinct strain range was selected for each group based on the inflection point where the curvature of the true stress-strain curve changed signs and the strain stiffening behavior ended. The inflection point was always found to be between 10 and 20 % strain. Subsequently, the Arruda-Boyce model parameters obtained by fitting the complete stress-strain dataset of the alginate groups and the stress-strain data ranging from 0 % to the respective inflection point of each curve for the gellan gum groups are presented in Table 3.

3.3. *Cell adhesion and mechanotransduction*

To evaluate cytocompatibility and compare how the different reinforcing networks affected cell behavior, we investigated the adhesion and spreading characteristics of adipose derived stromal cells (ADSCs)

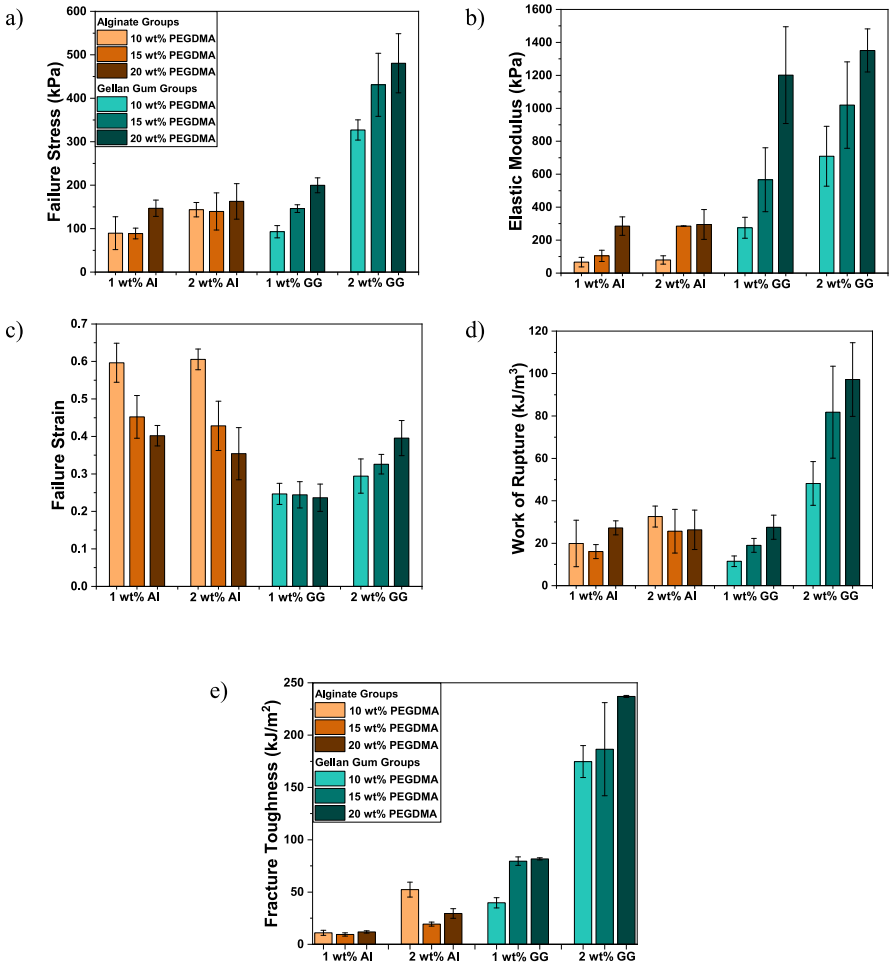

Fig. 5. Average mechanical properties of DN hydrogel groups: a) failure stress, b) elastic strain, c) failure strain, d) work of rupture, e) fracture toughness. The error bars represent one standard deviation.

Table 2
Comparison of the mechanical properties of 10 wt% PEGDMA + 1 wt% Al and 10 wt% PEGDMA + 1 wt% GG DN hydrogels tested using 0.5 mm/min and 5 mm/min displacement rates. Different superscripts in each column indicate significant difference ($p < 0.05$).

Reinforcing Network	Stretching Rate	Failure Stress (kPa)	Failure Strain	Elastic Modulus (kPa)	Work of Rupture (kJ/m^3)
Alginate	0.5 mm/min	81.4 ± 38^{a}	0.6 ± 0.05^{c}	66.74 ± 29^{f}	21.2 ± 10^{i}
	5 mm/min	87.8 ± 20^{a}	0.54 ± 0.04^{c}	65.6 ± 33^{f}	18.2 ± 3^{i}
Gellan gum	0.5 mm/min	90.3 ± 13^{a}	0.23 ± 0.03^{d}	270 ± 24^{g}	10.85 ± 3^{j}
	5 mm/min	135.2 ± 4^{b}	0.33 ± 0.02^{e}	218.8 ± 19^{h}	20.24 ± 1^{i}

on these hydrogels. ADSCs are a good model system for developing materials for biomedical implants and tissue engineering since they can be easily harvested from adipose tissue and show multipotency towards fat, cartilage, tendon, bone and potentially other tissues. We selected the 10 kDa poly(ethylene glycol) dimethacrylate (PEGDMA) hydrogels, which exhibit large difference in modulus when incorporating 1 wt% gellan gum ~275 kPa in comparison to 1 wt% alginate ~67 kPa. As depicted in Fig. 6a, cells cultured on 1 % gellan gum hydrogels displayed significantly greater spreading on day 7 compared to the 1 % alginate counterparts (17057 μm^2 and 9589 μm^2, respectively, in 1 % gellan gum and 1 % alginate samples). Moreover, we found a significant increase in molecular mechanosensory Yes-associated protein (YAP) nuclear localization in the gellan-gum incorporated samples: 21 % for cells adherent to 1 wt% alginate samples and 48 % for cells adherent to 1 wt% gellan gum samples, suggesting the mechanical properties of the networks are being sensed by the cell adhesion machinery with propagation to the nucleus.

4. Discussion

Previous studies of alginate and gellan gum reinforced DN PEG-based hydrogels have been conducted by various different research groups using various synthesis and test procedures, making side-by-side comparisons impossible (Huang et al., 2022; Pacelli et al., 2014; Trucco et al., 2021). In the present work, the different reinforcing networks of alginate and gellan gum were found to have distinct effects in controlling the mechanical and biological performance of DN PEG-based hydrogels. Each of these reinforcing networks provide unique characteristics to the DN hydrogels that will be discussed below.

4.1. Mechanical behavior of double network hydrogels

Gellan gum reinforced DN hydrogels generally demonstrated superior strength and stiffness in comparison to alginate reinforced DN hydrogels when the PEGDMA network variables were held constant

Table 3
Results of the Arruda-Boyce model fitting parameters for each group.

PEGDMA	Second Network	Swelling Stretch	Swollen $n \times 10^{24}$ [m^{-3}]	Swollen N	As fabricated $n \times 10^{24}$ [m^{-3}]	As fabricated N
10 wt%	1 wt% alginate	1.059	3.04	2.32	3.61	2.6
15 wt%		1.065	4.45	2.01	5.38	2.27
20 wt%		1.126	8	1.815	11.43	2.3
10 wt%	2 wt% alginate	1.017	4.94	3.04	5.2	3.15
15 wt%		1.058	7.83	1.97	9.27	2.21
20 wt%		1.094	8.71	1.53	11.4	1.83
10 wt%	1 wt% gellan gum	1.012	0.15	0.95	0.16	0.97
15 wt%		1.012	0.94	0.95	0.97	0.98
20 wt%		1.028	0.98	0.95	1.07	1
10 wt%	2 wt% gellan gum	1.01	1.93	0.96	1.99	0.98
15 wt%		1.01	2.9	0.96	3	0.98
20 wt%		1.024	3.6	0.97	3.87	1

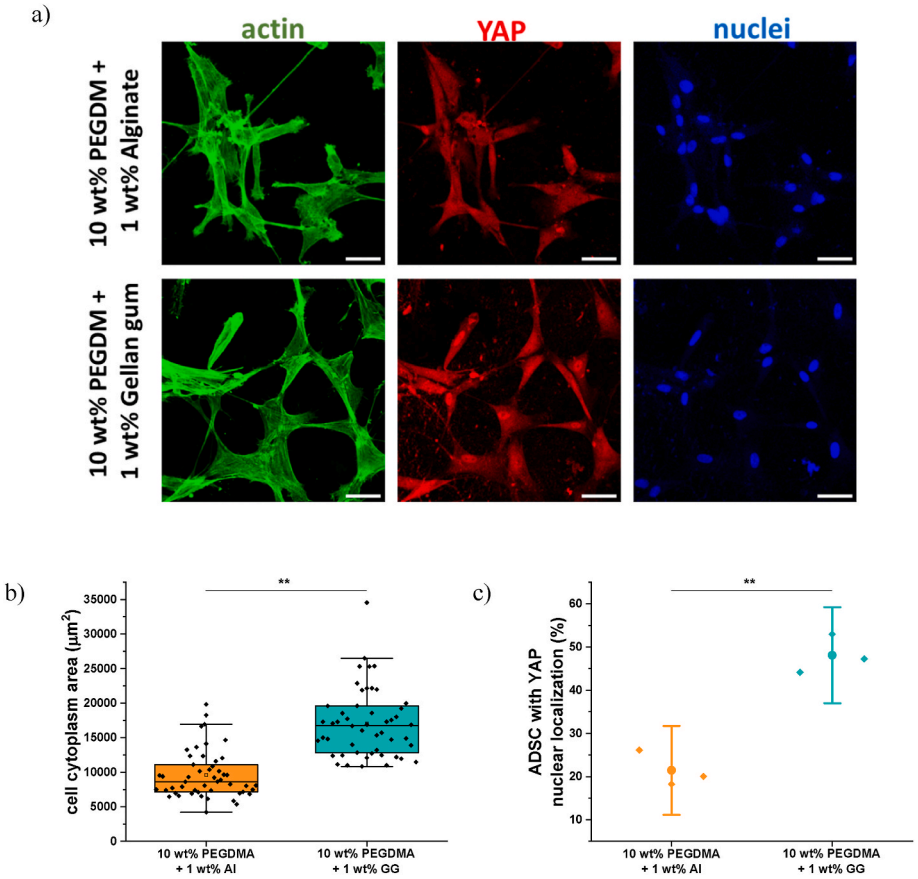

Fig. 6. a) Representative confocal images of ADSCs cultured on different hydrogel samples (scale bar = 50 μm), b) quantification of average cell area (n = 50, number of cells). ("**" represents $p < 0.01$ in one-way ANOVA test.), and c) quantification of YAP nuclear localization at day 7 ("**" represents $p < 0.01$ in one-way ANOVA test, n = 3. Total number of samples).

(Fig. 5a and b). An improvement of both strength and stiffness was also generally observed by increasing the concentration of PEGDMA and/or the reinforcing network. This enhancement is attributed to the rise in the effective hydrogel crosslinking density associated with higher concentrations of PEGDMA and/or the reinforcing network, as indicated by the higher "n" values in Table 3. The greater number of covalent and physical crosslinks formed due to the increased PEGDMA and/or the reinforcing network concentrations tends to make hydrogels more rigid. Regarding the strength, adding more reinforcing network takes stress off of the more brittle covalent network such that the DN hydrogel exhibits increasing strength with increasing reinforcing network concentration. These findings are generally consistent with previous studies (Huang et al., 2022; Li et al., 2014; Liu et al., 2020). Interestingly, for the 2 wt% alginate group, the high concentration of the reinforcing network rendered the PEGDMA concentration irrelevant to the strength, which has also been previously found in another study (Huang et al., 2022). This implies the strength behavior of the 2 wt% alginate group is fully determined by the alginate network.

A noticeably higher work of rupture and fracture toughness was observed for most of the gellan gum groups compared to the corresponding alginate groups (Fig. 5d and e). Furthermore, the work of rupture and fracture toughness results follow similar trends. For the gellan gum groups, there is a consistent enhancement in both the work of rupture and fracture toughness values as the concentrations of PEGDMA and/or gellan gum increase. For the alginate groups, the work of rupture and fracture toughness of hydrogels formed with alginate remains unaffected by an increase in PEGDMA concentration at 1 wt% alginate as the increase in strength is offset by a loss in stretchability. At

2 wt% alginate, the loss of stretchability dominates to give a decrease in work of rupture and fracture toughness with an increase in PEGDMA concentration. It is also noteworthy that such a direct, side-by-side comparison of these two different hydrogel toughness measurements has not been previously reported. Fig. 7 shows the fairly strong correlation between the notched sample fracture toughness and the unnotched sample work of rupture for a single reinforcement network type. This correlation was stronger for the gellan gum reinforcement, with an R^2 value of 0.93, and somewhat weaker for the alginate reinforcement, with an R^2 value of 0.78. However, gellan gum reinforcement clearly gives high fracture toughness than alginate reinforcement at each measured work of rupture value. Thus, performing the additional notched fracture toughness experiments is important for understanding the full mechanical response when comparing different tough DN hydrogel systems.

In contrast to the above properties, we found that alginate reinforced DN hydrogels generally exhibited greater stretchability compared to gellan gum reinforced DN hydrogels when the PEGDMA network variables were held constant (Fig. 5c). However, the difference between the two reinforcing networks was diminished as the amount of PEGDMA increased. This is attributed, in part, to the increased swelling in the alginate reinforced hydrogels with increased PEGDMA (Fig. 3a) that leads to chains that are more stretched at the start of the tensile experiment, thus reducing their capacity for further deformation and stretching. The observed trend of decreased stretchability for the alginate reinforced DN hydrogels with increasing concentrations of PEGDMA can also be attributed to the increasing number of effective crosslinks "*n*" and decreasing number of Kuhn segments between crosslinks "*N*" with increasing PEGDMA concentration (Table 3), indicating a tighter mesh in the network structure. This trend is similar to what was observed for the compressive strain to failure in alginate-PEG diacrylate DN hydrogels (Huang et al., 2022). Similarly, it was found that increasing the concentration of alginate had no significant effect on the tensile failure strain which is also consistent with previous compression failure strain results (Huang et al., 2022). In contrast, for the gellan gum-PEGDMA DN hydrogels, increasing the concentration of gellan gum significantly enhanced the stretchability of gellan gum-PEGDMA DN hydrogels as a higher concentration of gellan gum forms a more interconnected network (higher "n") without sacrificing the number of Kuhn segments between crosslinks "N." This observation aligns with several studies that have reported enhanced stretchability of various gellan gum DN hydrogels with increasing gellan gum concentration (Gao et al., 2023; Wen et al., 2014).

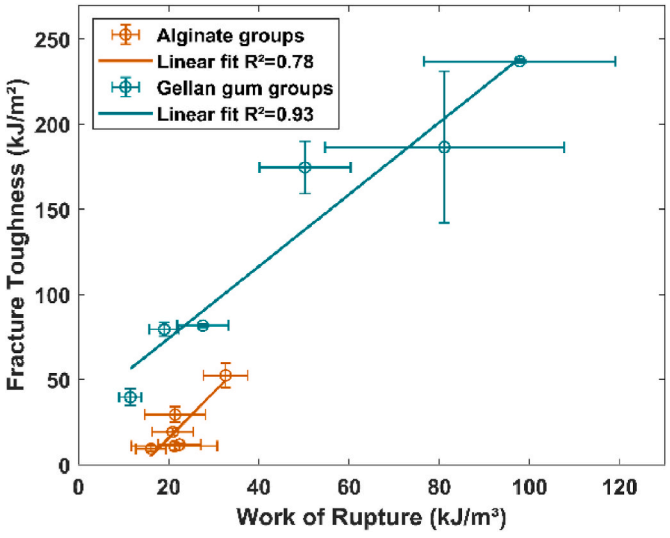

Fig. 7. Correlations of the notched sample fracture toughness values to the unnotched sample work of rupture values.

Finally, regarding the strain rate, we observed that alginate group exhibited comparable tensile responses under both strain rates, consistent with the findings of a previous study under compression loading (Huang et al., 2022). In contrast, the gellan gum group displayed somewhat lower initial modulus and increased failure strain and failure stress under the higher strain rate (Fig. 4c and Table 2). Thus, it appears the failure of the gellan gum network is more rate dependent than alginate, and the slower strain rate allows more time for the physical bonding to unzip and cause earlier failure.

4.2. Cell behavior on double network hydrogels

Our study reveals that gellan gum reinforced DN hydrogels with higher modulus significantly enhance ADSC spreading compared to alginate reinforced DN hydrogels (Fig. 6). The observed increase in cell spread area aligns with mechanotransduction principles, indicating that substrate stiffness influences cell adhesion and cytoskeletal tension, leading to increased spreading (Zhang et al., 2017). Furthermore, our findings reveal a significant rise in YAP nuclear localization on gellan gum hydrogels compared to alginate hydrogels, demonstrating the connection between hydrogel modulus, cell spreading, and YAP activation. Previous studies have demonstrated that the differentiation of ADSCs can be directed through changes in substrate stiffness using mechanotransduction networks from the matrix to the nucleus (Caliari et al., 2016; Yang et al., 2014). YAP is a transcriptional regulator whose subcellular localization between the cytoplasm and the nucleus conveys the attributes of mechanical microenvironments, which has been implicated in directing gene expression programs including differentiation. Given the substantial increases in cell area from the relatively lower modulus alginate reinforced samples to higher modulus gellan gum reinforced samples in our study, we examined whether cell spreading influences YAP activity in ADSCs. As illustrated in Fig. 6b, YAP primarily localizes to the cytoplasm in cells adherent to alginate-PEGDMA hydrogels. In contrast, there is an increase in nuclear YAP localization when cells are adherent to the gellan gum-PEGDMA hydrogels, suggesting the mechanical properties of the materials are differentially directing translocation of YAP. Collectively, these experiments demonstrate how the mechanical properties of DN hydrogels can guide mechanotransduction, which will prove useful for the design of biomedical materials that coax adherent cells to undergo a desired lineage specification.

4.3. Design insights for double network hydrogels

Based on the above results, it is clear that gellan gum reinforced DN hydrogels possess relatively higher strength, stiffness, toughness, and bioactivity towards cell lineages that are mechanoresponsive. Thus, gellan gum reinforced DN hydrogels would be preferred over alginate for tissue engineering scaffolds where a higher stiffness promotes lineage specific mechanotranscution, e.g., such as for musculoskeletal tissue like tendon and bone. Furthermore, the elastic modulus range of the gellan gum reinforced DN hydrogels overlaps that of cartilage, 1000–1500 kPa (Handorf et al., 2015), which should make them more suitable for cartilage repair or replacement applications. Another area of interest for DN hydrogels is soft robotics, where higher strength, stiffness, and toughness can be useful in actuator and other load bearing applications (Lee et al., 2020). In contrast, alginate-reinforced DN hydrogels will hold an advantage where lower modulus, high stretchability, and/or low strain rate sensitivity is desired. For example, the lower modulus range overlaps better with soft tissues, such as fat and muscle, and in tissues where stretchability is an essential characteristic, such as intestine and arteries (Akhtar et al., 2011; Handorf et al., 2015). Furthermore, the field of soft robotics requires low modulus and stretchability for various applications such as sensors and circuit board substrates (Lee et al., 2020). Overall, the results of this study provide DN materials with a broad range of mechanical characteristics and new

insights regarding double network hydrogel design criteria for specific property requirements.

5. Conclusions

This study provides direct comparisons of the mechanical abd biologican properties of PEG-based double network hydrogels reinforced with sodium alginate versus gellan gum networks. Gellan gum reinforcement of PEGDMA resulted in double network (DN) hydrogels with higher strength, stiffness, work of rupture, and fracture toughness compared to those reinforced with an identical amount of alginate. The increased modulus in the gellan gum reinforced DN hydrogels contributes to increased cell spreading and controlled activation of mechanosensory elements. In contrast, the alginate reinforced DN hydrogels demonstrated higher stretchability. However, this stretchability advantage was significantly diminished at higher mass fractions of PEGDMA where higher swelling and a tighter effective network mesh reduced the stretchability, a benefit that diminished with increasing mass fractions of PEGDMA due to higher swelling and a tighter effective network mesh. Higher strain rates demonstrated no significant impact on the mechanical properties of alginate reinforced DN hydrogels, while they enhanced the strain and stress to failure for the gellan gum reinforced DN hydrogels. This is attributed to the failure and unzipping of physical bonds within the gellan gum network being more rate dependent than for alginate.

Side-by-side comparison between work of rupture and fracture toughness revealed consistent trends in both properties with changing mass fraction of PEGDMA, reinforcing network type, and reinforcing network mass fraction. However, when comparing between the groups gellan gum reinforcement clearly gives higher fracture toughness than alginate reinforcement at each measured work of rupture value. This result highlights the importance of conducting additional notched fracture toughness experiments in order to fully understand the mechanical response when comparing different tough DN hydrogel systems.

Overall, gellan gum reinforced DN hydrogels should be preferred for applications that require high strength, stiffness, toughness, and/or bioactivity towards lineages that are mechanoresponsive. In contrast, alginate reinforced DN hydrogels appear to hold the advantage where low modulus, high stretchability, and/or low strain rate sensitivity is desired. Empowered by this knowledge, researchers can make informed decisions when designing double network hydrogels for various applications with different specific property requirements.

CRediT authorship contribution statement

Alaa Ajam: Writing – review & editing, Writing – original draft, Methodology, Investigation, Formal analysis. **Yuwan Huang:** Writing – review & editing, Methodology, Investigation. **Md Shariful Islam:** Writing – review & editing, Methodology, Investigation. **Kristopher A. Kilian:** Writing – review & editing, Supervision, Methodology, Funding acquisition, Conceptualization. **Jamie J. Kruzic:** Writing – review & editing, Writing – original draft, Supervision, Project administration, Methodology, Funding acquisition, Conceptualization.

Declaration of competing interest

The authors declare that they have no known competing financial interests or personal relationships that could have appeared to influence the work reported in this paper.

Data availability

Data will be made available on request.

Acknowledgements

The authors thank Dr. Meredith Silberstein for helpful discussions and they acknowledge the use of the facilities provided by the Mark Wainwright Analytical Centre at the University of New South Wales. Financial support was provided by the Australian Research Council grant DP210103654.

Appendix A. Supplementary data

Supplementary data to this article can be found online at https://doi.org/10.1016/j.jmbbm.2024.106642.

References

Akhtar, R., Sherratt, M.J., Cruickshank, J.K., Derby, B., 2011. Characterizing the elastic properties of tissues. Mater. Today 14, 96–105.
Arruda, E.M., Boyce, M.C., 1993. A three-dimensional constitutive model for the large stretch behavior of rubber elastic materials. J. Mech. Phys. Solid. 41, 389–412.
Caliari, S.R., Vega, S.L., Kwon, M., Soulas, E.M., Burdick, J.A., 2016. Dimensionality and spreading influence MSC YAP/TAZ signaling in hydrogel environments. Biomaterials 103, 314–323.
Caló, E., Khutoryanskiy, V.V., 2015. Biomedical applications of hydrogels: a review of patents and commercial products. Eur. Polym. J. 65, 252–267.
Ferris, C., Stevens, L., Gilmore, K.J., Mume, E., Greguric, I., Kirchmajer, D., Wallace, G. G., 2015. Peptide modification of purified gellan gum. J. Mater. Chem. B 3, 1106–1115.
Gao, Y., Zhou, J., Xu, F., Huang, W., Ma, X., Dou, Q., Fang, Y., Wu, L., 2023. Highly stretchable, self-healable and self-adhesive double-network eutectogel based on gellan gum and polymerizable deep eutectic solvent for strain sensing. ChemistrySelect 8, e202204463.
Handorf, A.M., Zhou, Y., Halanski, M.A., Li, W.-J., 2015. Tissue stiffness dictates development, homeostasis, and disease progression. Organogenesis 11, 1–15.
Hong, S., Sycks, D., Chan, H.F., Lin, S., Lopez, G.P., Guilak, F., Leong, K.W., Zhao, X., 2015. 3D printing of highly stretchable and tough hydrogels into complex, cellularized structures. Adv. Mater. 27, 4035–4040.
Huang, Y., Jayathilaka, P.B., Islam, M.S., Tanaka, C.B., Silberstein, M.N., Kilian, K.A., Kruzic, J.J., 2022. Structural aspects controlling the mechanical and biological properties of tough, double network hydrogels. Acta Biomater. 138, 301–312.
Huey, D.J., Hu, J.C., Athanasiou, K.A., 2012. Unlike bone, cartilage regeneration remains elusive. Science 338, 917–921.
Islam, M.S., Molley, T.G., Ireland, J., Kruzic, J.J., Kilian, K.A., 2021. Magnetic nanocomposite hydrogels for directing myofibroblast activity in adipose-derived stem cells. Advanced NanoBiomed Research 1, 2000072.
Lee, K.Y., Mooney, D.J., 2012. Alginate: properties and biomedical applications. Prog. Polym. Sci. 37, 106–126.
Lee, S., Tong, X.M., Yang, F., 2014. The effects of varying poly(ethylene glycol) hydrogel crosslinking density and the crosslinking mechanism on protein accumulation in three-dimensional hydrogels. Acta Biomater. 10, 4167–4174.
Lee, Y., Song, W.J., Sun, J.Y., 2020. Hydrogel soft robotics. Mater Today Phys 15, 100258.
Li, J., Illeperuma, W.R.K., Suo, Z., Vlassak, J.J., 2014. Hybrid hydrogels with extremely high stiffness and toughness. ACS Macro Lett. 3, 520–523.
Li, W., Wu, D., Hu, D., Zhu, S., Pan, C., Jiao, Y., Li, L., Luo, B., Zhou, C., Lu, L., 2020. Stress-relaxing double-network hydrogel for chondrogenic differentiation of stem cells. Mater. Sci. Eng., C 107, 110333.
Lin, C.-C., Metters, A.T., 2006. Hydrogels in controlled release formulations: network design and mathematical modeling. Adv. Drug Deliv. Rev. 58, 1379–1408.
Lin, C.C., Anseth, K.S., 2009. PEG hydrogels for the controlled release of biomolecules in regenerative medicine. Pharm. Res. (N. Y.) 26, 631–643.
Liu, S., Qiu, Y., Yu, W., Zhang, H., 2020. Highly stretchable and self-healing strain sensor based on gellan gum hybrid hydrogel for human motion monitoring. ACS Appl. Polym. Mater. 2, 1325–1334.
Matsuda, T., Kawakami, R., Namba, R., Nakajima, T., Gong, J.P., 2019. Mechanoresponsive self-growing hydrogels inspired by muscle training. Science 363, 504–508.
Nguyen, Q.T., Hwang, Y., Chen, A.C., Varghese, S., Sah, R.L., 2012. Cartilage-like mechanical properties of poly (ethylene glycol)-diacrylate hydrogels. Biomaterials 33, 6682–6690.
Pacelli, S., Paolicelli, P., Pepi, F., Garzoli, S., Polini, A., Tita, B., Vitalone, A., Casadei, M. A., 2014. Gellan gum and polyethylene glycol dimethacrylate double network hydrogels with improved mechanical properties. J. Polym. Res. 21, 1–13.
Pal, K., Banthia, A.K., Majumdar, D.K., 2009. Polymeric hydrogels: characterization and biomedical applications. Des. Monomers Polym. 12, 197–220.
Peppas, N.A., Bures, P., Leobandung, W., Ichikawa, H., 2000. Hydrogels in pharmaceutical formulations. Eur. J. Pharm. Biopharm. 50, 27–46.
Rivlin, R.S., Thomas, A.G., 1953. Rupture of rubber. I. Characteristic energy for tearing. J. Polym. Sci. 10, 291–318.
Rowley, J.A., Madlambayan, G., Mooney, D.J., 1999. Alginate hydrogels as synthetic extracellular matrix materials. Biomaterials 20, 45–53.
Trucco, D., Vannozzi, L., Teblum, E., Telkhozhayeva, M., Nessim, G.D., Affatato, S., Al-Haddad, H., Lisignoli, G., Ricotti, L., 2021. Graphene oxide-doped gellan

gum–PEGDA bilayered hydrogel mimicking the mechanical and lubrication properties of articular cartilage. Adv. Healthcare Mater. 10, 2001434.
Uchida, M., Sengoku, T., Kaneko, Y., Okumura, D., Tanaka, H., Ida, S., 2019. Evaluation of the effects of cross-linking and swelling on the mechanical behaviors of hydrogels using the digital image correlation method. Soft Matter 15, 3389–3396.
Wen, C., Lu, L., Li, X., 2014. An interpenetrating network biohydrogel of gelatin and gellan gum by using a combination of enzymatic and ionic crosslinking approaches. Polym. Int. 63, 1643–1649.
Yang, C., Tibbitt, M.W., Basta, L., Anseth, K.S., 2014. Mechanical memory and dosing influence stem cell fate. Nat. Mater. 13, 645–652.
Zhang, Q., Lin, S., Li, Q., Zhao, D., Cai, X., 2017. Cellular response to surface topography and substrate stiffness. Cartilage Regeneration 41–57.
Zhou, W., Zhang, H., Liu, Y., Zou, X., Shi, J., Zhao, Y., Ye, Y., Yu, Y., Guo, J., 2019. Preparation of calcium alginate/polyethylene glycol acrylate double network fiber with excellent properties by dynamic molding method. Carbohydr. Polym. 226, 115277.
Zhou, W., Zhang, H., Liu, Y., Zou, X., Shi, J., Zhao, Y., Ye, Y., Yu, Y., Guo, J., 2020. Sodium alginate-polyethylene glycol diacrylate based double network fiber: rheological properties of fiber forming solution with semi-interpenetrating network structure. Int. J. Biol. Macromol. 142, 535–544.
Zia, K.M., Tabasum, S., Khan, M.F., Akram, N., Akhter, N., Noreen, A., Zuber, M., 2018. Recent trends on gellan gum blends with natural and synthetic polymers: a review. Int. J. Biol. Macromol. 109, 1068–1087.